JACS
JOURNAL OF THE AMERICAN CHEMICAL SOCIETY
Article
pubs.acs.org/JACS

Quantum Dots as Templates for Self-Assembly of Photoswitchable Polymers: Small, Dual-Color Nanoparticles Capable of Facile Photomodulation

Sebastián A. Díaz,[⊥,‡] Luciana Giordano,[⊥] Julio C. Azcárate,[§] Thomas M. Jovin,*[,⊥] and Elizabeth A. Jares-Erijman[‡,†]

[⊥]Laboratory of Cellular Dynamics, Max Planck Institute for Biophysical Chemistry, Am Fassberg 11, 37077 Göttingen, Germany

[‡]Departamento de Química Orgánica, Facultad de Ciencias Exactas y Naturales, Universidad de Buenos Aires, CIHIDECAR, CONICET, 1428 Buenos Aires, Argentina

[§]Instituto de Investigaciones Fisicoquímicas Teóricas y Aplicadas, Facultad de Ciencias Exactas, Universidad Nacional de La Plata, CONICET, La Plata, Argentina

ABSTRACT: A photomodulatable amphiphilic polymer has been synthesized with a backbone of poly[isobutylene-*alt*-maleic anhydride] and pendant dodecyl alkyl chains, Lucifer Yellow (LY) fluorescent probes, and diheteroarylethenes photochromic (PC) groups. The latter serve as reversible UV-activated FRET acceptors for the LY donors. We characterized the spectral and switching properties of the polymer in an organic solvent ($CHCl_3$). In an aqueous medium the polymer forms polymersomes, constituting fluorescence probes ~75 nm in diameter. Self-assembly of the polymer on the surface of a quantum dot (QD) serving as a template creates a dual-color photoswitchable nanoparticle (psNP) with improved properties due to the increase in polymer density and efficiency of PC photoconversion. The psNP exhibits a second QD red emission band that functions as an internal standard requiring only a single excitation wavelength, and is much reduced in size (<20 nm diameter) compared to the polymersomes. The QD template also greatly increases the depth of modulation by photochromic FRET of the LY emission monitored by both steady-state and time-resolved (lifetime) fluorescence (from 20%→70%, and from 12%→55%, respectively).

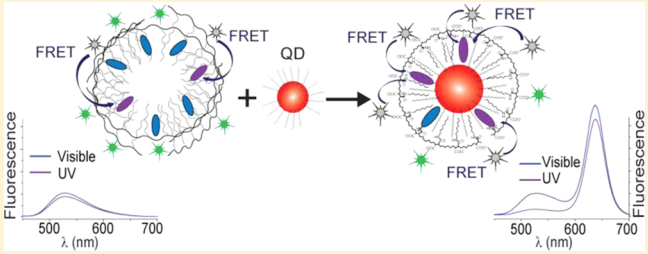

1. INTRODUCTION

Nanoparticles (NPs) employed as imaging probes are indispensable tools for the observation of biological systems.[1,2] NPs can be organic [polymersomes, dendrimers, polymeric nanocapsules][3] or primarily inorganic, as in the case of metallic [Au, Ag, Pt],[4] magnetic [Fe_3O_4],[4] silica based [SiO_2],[4] and semiconductor nanocrystals (quantum dots, QDs).[5] They can be modified and functionalized so as to provide unique properties, particularly for imaging strategies based on fluorescence, radioactivity, or NMR spectroscopy.[6−8] QDs exhibit excellent inherent properties as fluorophores (broad excitation, narrow emission, photostability, and brightness),[5] enabling applications impossible with other probes.[9]

An interesting property of fluorescent probes is their potential for systematic modulation of one or more specific parameters, for example emission intensity.[10,11] Numerous modulatable probes have been developed for enhancing selective detection by suppression of background contributions and degradation by photobleaching.[12−15] By satisfying certain spectroscopic and structural criteria, Förster resonance energy transfer (FRET) can be employed as an efficient means for generating modulation of fluorescence.[16−18] Of particular interest are probes whose emission can be controlled by an external light source.[19−21] Photochromic (PC) molecules, e.g., diheteroarylethenes, function well as versatile acceptors, creating FRET pairs that can be switched between transfer/nontransfer states by light.[22,23] Reversible FRET based on photochromic acceptors, which we have denoted as photochromic FRET (pcFRET),[22] has been exploited in a variety of systems, including those based on nanoparticles.[24,25]

Diheteroarylethenes present many advantages in pcFRET-based strategies (fatigue resistance, lack of thermal conversion, high photoconversion efficiencies, and controlled tailoring of optical properties through chemical modification),[26] but their efficient operation is generally limited to nonpolar media.[27] This limitation has been overcome by creating NPs with amphiphilic properties, providing water solubility and at the same time a nonpolar internal compartment in which the PC can be placed.[28−32] In the original publication on pcFRET, Giordano et al.[22] demonstrated the applicability of diheteroarylethenes as acceptors for the donor Lucifer Yellow (LY) in organic solvents. In the present study, the same FRET pair was used, but the donor and acceptor were covalently bound to an

Received: December 6, 2012
Published: January 29, 2013

 © 2013 American Chemical Society dx.doi.org/10.1021/ja3117813 | *J. Am. Chem. Soc.* 2013, 135, 3208−3217

Scheme 1. (A) Chemical Components of Polymer Preparation; (B) Schematic Representation of Polymer and Subsequent NP Preparation

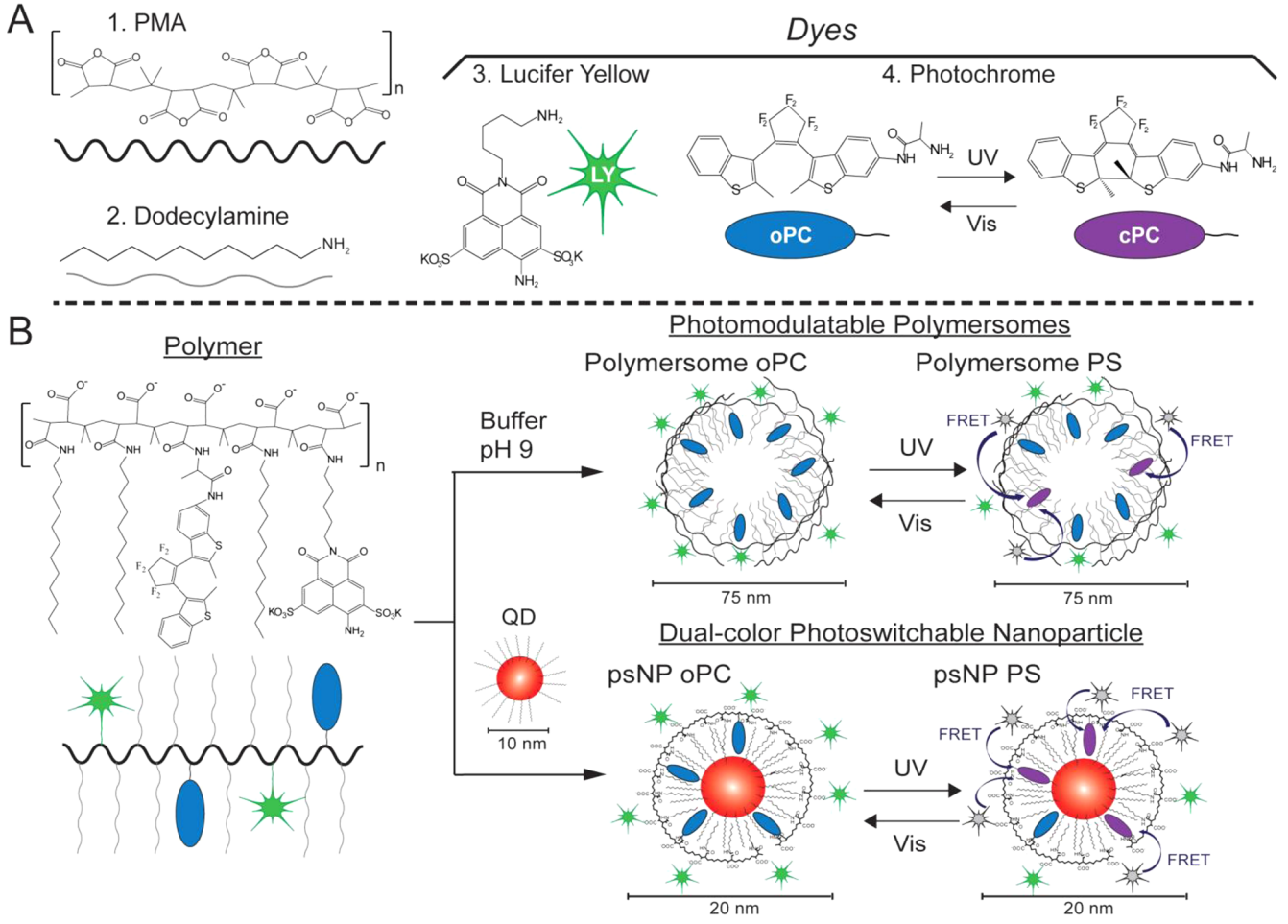

amphiphilic polymer to create dual polarity NPs in the form of polymersomes, thereby overcoming the requirement for an organic solvent. The system provides the additional advantages of the greater fluorescence quantum yield and photostability provided by the attachment of multiple probes to the same polymeric support.[3]

QDs also present limitations similar to those of PC molecules, in that they are generally prepared in organic solvents and carry surface ligands that must be exchanged or capped to gain water solubility.[33] The capping methodology first introduced by Pellegrino et al.[34] offers an elegant means for solubilizing both QDs and the PC moieties. An amphiphilic polymer based on a poly[isobutylene-*alt*-maleic anhydride] backbone (PMA) with pendant photochromic groups renders the QDs water-soluble and at the same time places the PC molecules within the hydrophobic microenvironment created between the polymer cap and the QD surface bearing organic ligands. We have used this architecture to modulate the fluorescence of QDs without[25] and with[35] a secondary reference probe.

There are many examples in the literature of micelles and polymer vesicles (polymersomes)[36] functioning as imaging agents.[3,37,38] Our intention was to establish the suitability of our photomodulatable polymers in such applications and in comparison with previous reagents.[39,40] We determined that a QD served very well as a template for the amphiphilic fluorescent photomodulatable polymer, thereby creating a new, improved probe. The QD template complements the LY emission (525 nm), providing a second emission color (635 nm), while retaining the single excitation wavelength, and reduces the diameter of the NP probe to 20 nm from the 75 nm of the polymersome preparation. The QD also greatly increases the PC-dependent modulation of the LY emission monitored by both steady-state and time-resolved (lifetime) fluorescence determinations (from 20%→70%, and 12%→55%, respectively). We attribute this circumstance to the greater polymer density and efficiency of PC photoconversion. The entire construct consisting of the photomodulatable polymer coating the red-emitting QD is referred to as a dual-color photoswitchable nanoparticle (psNP).

2. RESULTS AND DISCUSSION

2.1. Polymer Synthesis and Nanoparticle Preparations. The specifics of polymer synthesis and psNP preparation are given in the Experimental Section. We present here the key conceptual aspects. We utilized a PMA polymer backbone because it is economical, available commercially, and can be modified directly by virtue of anhydride groups that react readily with primary amines to form covalent amide bonds.[41] To create the photomodulatable micelles we modified the polymer by conjugation with alkyl chains (dodecylamine), PC molecules acting as FRET acceptors, and Lucifer Yellow Cadaverine as the fluorescent donor. All three constituent

dx.doi.org/10.1021/ja3117813 | J. Am. Chem. Soc. 2013, 135, 3208−3217

molecules carry primary amine linker groups. The PC was [2-amino-N-(3-(3,3,4,4,5,5-hexafluoro-2-(2-methylbenzo[*b*]-thiophen-3-yl)cyclopent-1-enyl)-2-methylbenzo[*b*]thiophen-6-yl)propanamide], a diheteroarylethene with an alanine linker. Compared to an aromatic amine, the short linker increases conjugation to the polymer while minimizing the distance to the LY on the polymer backbone.[42] The protocol for polymer synthesis has been thoroughly described in the literature.[34,41] Our preparation conditions were slightly modified (Scheme 1) in order to satisfy the requirement for different solvents in forming the PC and fluorescent adducts.

The coating of the QD with the polymer was by a self-assembly mechanism directed by the hydrophobic interactions of the alkyl chains of the polymer with the surface ligands of the QD.[34] The carboxyl groups, which are formed by the nucleophilic attack on the anhydride groups by either the amines or water molecules, orient externally and provide the negative charge stabilizing the psNP in buffer solution. The typical polymer comprised ~40 monomers. The distribution of the dyes on the polymer and that of the polymers on the QD are presumed to be random. The number of polymers per QD has been demonstrated previously as being critical for forming stable nanoparticles while avoiding excess empty polymersomes so as to facilitate purification procedures.[25,43]

2.2. Comparison of Polymer in Organic Solvent to the Polymersomes in Buffer. The purified polymer was characterized using absorbance spectroscopy. To understand the basis for this procedure we provide a photophysical description of the PC molecule, which appears not to be modified by its conjugation to the polymer. The PC can exist in two states, the open form (oPC), which can assume both parallel and antiparallel conformations, and the photocyclized closed form (cPC), obtained upon irradiation of the oPC with UV light.[26] Back conversion to the oPC form in ~100% yield is accomplished by exposure to green light (typically 545 ± 10 nm), which is only absorbed by cPC. In contrast, the formation of cPC is incomplete due to (i) the photoreversal that occurs upon excitation of cPC, which also absorbs in the UV, and (ii) the restriction of photoconversion to the antiparallel conformation of oPC.[44] Thus, UV irradiation leads to a photostationary state (PS) that depends solely on the wavelength (but not the intensity) of UV irradiation and the local environment of the PC groups.[35,45] In the experiments presented below, exposure to UV light (340 ± 10 nm) led to a fractional cPC content in the photostationary state, α_{PS} = cPC/(cPC + oPC), of 0.22; this quantity was determined from the increase in A_{540}.[35] The concentration of total PC was determined from α_{PS} and the known differences in extinction coefficients, while the LY concentration was calculated from A_{430} after correcting for the contributions of the PC and scattering by the polymer.

Based on the above determinations, the final polymer (designated as PMA 9PC 75C12 2.5LY) contained for every 1000 original isobutylene-*alt*-maleic anhydride monomers, 90 PC molecules, 750 dodecylamine chains, and 25 LY. From the α_{PS} of 0.22, we infer a ~1−1.25 ratio of acceptors (cPC) to donors (LY), i.e. close to the design goal of a 1:1 stoichiometry.

The LY−PC pair is an effective pcFRET pair in organic solvents,[22] and we assessed whether the FRET process operated with unimpaired properties in the case of the polymer in $CHCl_3$. The spectral properties are given in Figure 1 and the corresponding calculations in Table 1. The parameters of greatest relevance for the probe are the quantum yield (QY),

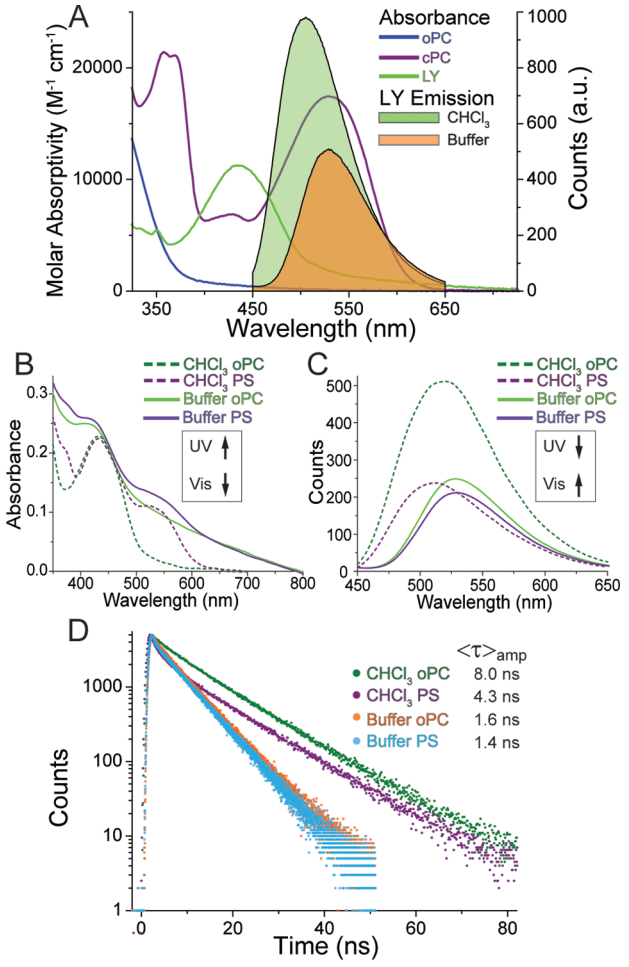

Figure 1. (A) Spectral overlap of absorbance (solid lines) and emission (filled areas) for PC and LY. The emission spectra are scaled so as to represent their respective QYs. (B−D) Spectroscopic monitoring of PMA 9PC 75C12 2.5LY in different solvents ($CHCl_3$ and buffer) and states (oPC and PS). Irradiation was: UV, 340 ± 10 nm (irradiance 1.1 mW cm^{-2}); vis, 545 ± 10 nm (6.2 mW cm^{-2}). Temperature, 20 °C. (B) Absorbance spectra. (C) Steady-state fluorescence, excitation at 420 nm. (D) Time-resolved fluorescence decays monitored at 530 nm. Excitation source, N-460 nanoLED.

the modulation of steady-state fluorescence (Quench %), the amplitude-weighed mean lifetime $\langle\tau\rangle_{amp}$, and its corresponding degree of modulation.[46] The aim of the study was to transfer the previously studied FRET pair to an aqueous medium. Thus, polymersomes were created by suspension of the polymer in 50 mM Na-borate buffer (SBB), pH 9. The properties changed dramatically, as can be seen in Table 1.

The larger QY, $\langle\tau\rangle_{amp}$, and the blue-shifted emission are attributable to the aprotic nonpolar environment provided by $CHCl_3$.[47] It is hypothesized that apolar solvents inhibit certain nonradiative decay mechanisms, thereby leading to an increase in both $\langle\tau\rangle_{amp}$ and QY.[47] The larger value of R_o in $CHCl_3$ compared to buffer is due to the greater QY of the LY (~2-fold increase), overcompensating a decrease in the overlap integral (J) of ~5%.[16]

The properties of LY are unmodified by conjugation to the polymer, such that the polymersomes offer a significant multiplexing advantage. However, of primary relevance to the proposed uses of photoswitchable probes are the attainable modulation of steady-state emission (quenching and dequench-

dx.doi.org/10.1021/ja3117813 | J. Am. Chem. Soc. 2013, 135, 3208−3217

Table 1. Properties of Photomodulatable Amphiphilic Polymer in $CHCl_3$ and SBB

polymer	LY-cPC R_o [nm][b]	emission peak [nm]	QY	quench [%]	$\langle\tau\rangle_{amp}$ [ns][c]	$\langle\tau\rangle_{amp}$ modulation [%]	cPC/LY in PS state	α_{PS}
in $CHCl_3$	4.4	502	0.47	60	8.0 ± 0.3	46	0.81 ± 0.01	0.22
polymersome	3.9	529	0.25	20	1.6 ± 0.2	13	0.20 ± 0.02	0.06
mixed polymer[a]	3.9	529	0.25	30	3.4 ± 0.3	21	0.55 ± 0.04	0.15

[a]Polymersomes formed with PMA 9PC 75C12 2.5LY mixed in a 1:1 ratio with PMA 75C12 (a polymer which contains only dodecylamine chains). [b]Förster transfer parameter (R_o); [c]Amplitude-weighed mean fluorescence lifetime; excitation source, N-460 nanoLED.

ing) and the corresponding change(s) in lifetime(s). These properties are those measured by lock-in detection imaging and FLIM.[48,49] Experiments with the pure polymer PMA 9PC 75C12 2.5LY in buffer solution provided disappointing initial results according to both measures. That is, the photomodulation decreased markedly from that observed in $CHCl_3$. We have previously suggested that the inclusion of numerous voluminous dye groups in amphiphilic polymers negatively alters the QD coating efficiency.[35] In the case of polymersomes, increasing the number of large dye molecules relative to the dodecylamine chains probably leads to greater water permeability, diminishing the hydrophobic character of the interior. The photostationary states of PC in polymers placed in organic solvents and aqueous solutions are similar if the polymersome is well formed and compact (α_{PS} ~0.22). However, α_{PS} for the polymersomes generated in the present study was lower by 73%, indicating that for PC molecules in a polar environment the extent of photoconversion induced by UV light diminishes greatly. Indeed, "dilution" of the composite polymer with a second polymer containing only dodecylamine chains (PMA 75C12) led to increases in all of the relevant properties (degree of quenching, cPC/LY ratio, and $\langle\tau\rangle_{amp}$ (mixed polymer in Table 1).

An additional consideration is the size of the various preparations. Measured by DLS the polymersome diameter had a broad distribution, 75 ± 35 nm. A large corresponding scattering contribution is also evident in Figure 1B. We conclude that although the polymersomes constitute bright tags by virtue of incorporating many LY fluorophores, they are too large for many applications. Furthermore, the degree of photomodulation, ≤20% according to both steady-state intensity and time-correlated fluorescence, is marginal.

2.3. Dual-Color Photoswitchable Nanoparticles. Metallic or semiconductor NPs soluble in organic solvents carry multiple organic ligands bound to the outer shell that control the NP size during synthesis and provide stability after completion of the reaction.[50] Typical examples in the case of QDs are trioctylphosphine oxide (TOPO), trioctylphosphine (TOP), and 1-hexadecylamine (HDA). All three ligands are present in the series A CSS 635 nm QDs CdSe/CdS/ZnS core−shell−shell nanoparticles[51] (CAN GmbH, Hamburg) utilized in our experiments. The coating of NPs containing such organic ligands with amphiphilic polymers is well documented in the literature.[33] Our previous publications demonstrated that the space between the QD surface and the polymer provides an excellent hydrophobic microenvironment for PC switching,[25,35] and it was anticipated that a NP template would enhance the properties exhibited by the polymersomes. By utilizing a QD with an emission at a longer wavelength we achieved the anticipated improvements in key parameters, and created a NP with the added advantage of a second emission band. These psNPs are suitable for ratiometric photomodulation, with the QD functioning as a very stable internal standard. In addition, the QDs can also be imaged independently by exciting at a wavelength beyond the spectral region of LY. Except for a slightly reduced intensity (QY) the desirable properties of the QD emission are maintained.

2.3.1. Physical Characterization. The psNPs were imaged by TEM. The measured diameter of the naked QD in organic solvent was 9.2 ± 0.6 nm and 9.9 ± 0.5 nm for the QDs coated with the PMA 9PC 75C12 2.5LY. Although the QD fluorescence prevented us from utilizing DLS to estimate a hydrodynamic radius, we inferred from FRET calculations a diameter in solution of ~18−19 nm (see section 2.3.2). This value is compatible with the reported ratio of the hydrodynamic/TEM radii of ~2.[52] Size exclusion chromatography yielded consistent results. Using an analytical Superdex-200 (GE Healthcare) column the empty polymersome component eluted consistently before the psNP fraction. The psNPs were stable for over 6 months, without demonstrable changes in properties, and exhibited resistance to pH changes in the range of 8−12 and a salt concentration lowered to 0.5 mM.

2.3.2. Spectral Characterization of the LY and QD Emission Components of psNP. The dual-color psNP was studied spectroscopically by absorbance, steady-state fluorescence, and TCSPC-monitored fluorescence decay.

Estimates were obtained from the absorbance spectra of the number of dyes and polymer chains coating each QD. The LY and PC concentrations were calculated in a manner similar to that that used in the characterization of the polymer (see section 2.2). Assigning A_{625} in the oPC state entirely to the QD, led to a determination of the QD concentration and, thereby, the psNP composition. In the PS state, there were 52 ± 2 LY from an equivalent number of polymer chains, and 35 ± 2 cPC (out of a total of ~190 PC) per QD. The large number of LY groups is important for two reasons. The first has to do with the much larger absorption cross-section (~150-fold) of the QD itself. With ~50 LYs per QD the probability of a photon being absorbed by LY at its absorption maximum of 430 nm, relative to that of absorption by the QD, is ~1: 3; i.e., out of 4 absorbed photons 3 will be by the QD and 1 by the LY. The second consideration is the capacity of the QD for acting as a FRET acceptor for the LY donor. In view of the very favorable R_o of 6.9 nm, FRET decreases the LY emission significantly.

The function of both the LY and the QD as FRET donors to the cPC acceptor leads to a globally more efficient cycloreversion of the cPC to the oPC form.[35,53] Assuming a homogeneous PC population we calculated a value of α_{PS} of 0.17−0.19, much higher than the 0.06 observed with polymersomes and similar to 0.22 in $CHCl_3$. We conclude that in the assembled psNP, the PC groups are located predominantly in the hydrophobic compartment defined by the QD surface and the overlying polymer cap. In contrast, the LY are external to the polymer coat and thus exposed to the aqueous medium.

dx.doi.org/10.1021/ja3117813 | J. Am. Chem. Soc. 2013, 135, 3208−3217

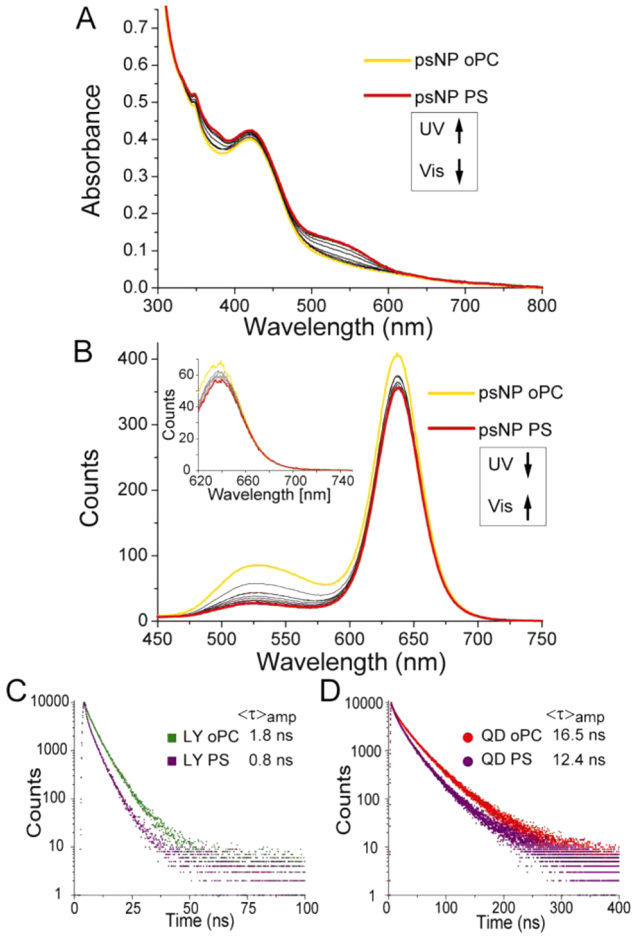

Figure 2. Spectroscopic monitoring of dual-color psNP. Irradiation was: UV, 340 ± 10 nm (irradiance 1.1 mW cm^{-2}); Vis, 545 ± 10 nm (6.2 mW cm^{-2}). Temperature, 20 °C. (A) Absorbance spectra. (B) Fluorescence spectra, excitation at 420 nm. Inset: Fluorescence spectra, excitation at 600 nm. (C,D) Time-resolved fluorescence decays. Excitation source, N-460 nanoLED; emission monitored at either 530 nm (C) or 635 nm (D).

Figure 2B,C demonstrates photomodulation of the LY on the psNPs, while panels B and D indicate that the QD emission also exhibited modulation (changes in lifetime) due to cycling the PC. Table 2 compares the relevant properties of the two emitting components in different situations.

Although the LY appeared to be exposed to the aqueous medium in both the psNP and the polymersomes, a certain number of groups may have been situated in the more hydrophobic microcompartment of the psNP, giving rise to the slight hypsochromic shift (∼4 nm) in the emission peak as well as the increase in mean lifetime.[47] The reduced QY probably reflects FRET from the LY to the QD, as discussed earlier. Using this assumption we calculate a mean r_{DA} (donor−acceptor distance),[16] of 9.2 nm for this process. Assuming that the LY are on the outer layer of the psNP, it follows that the diameter of psNP in solution is 18−19 nm. The primary observation was the large increase in both steady-state quenching and lifetime modulation of the LY on the psNP, which we attributed to two main factors, the first being the larger α_{PS} obtained by placing the PC in the hydrophobic microenvironment. The almost 3-fold greater number of cPC per LY implies an equivalent increase in the acceptor cross-section. A second factor is the reduced size of the final NP, with the QD acting as a more efficient template for concentrating the polymer. The reduced surface area and higher acceptor surface density lead to more efficient intermolecular FRET between neighboring polymers. This phenomenon is also documented by a quantitative comparison of the FRET parameters for the PMA polymer in $CHCl_3$ solution or incorporated into the psNP (see Spectral Kinetics and FRET Systems).

The properties of the QD component of the psNP are summarized in the lower half of Table 2, in which a comparison is made with QDs coated with a polymer containing only dodecylamine chains, i.e. lacking PC. We attribute the reduction in QY and lifetime to a lower coating efficiency of the QD with the polymer containing voluminous dye groups.[35] QDs lacking such moieties exhibit a greater QY, comparable to that in organic solvents such as $CHCl_3$.[25] We observed a small change in the QD fluorescence (12%) upon UV irradiation of the psNP. In the case of excitation wavelengths at which the LY absorbance was considerable, the QD quenching was as high as 14%. The R_o for the isolated QD−cPC donor−acceptor pair is only 2.3 nm, such that little discernible FRET was expected. Yet, due to the 35 acceptors present in the PS state the effective R_o would be $35^{1/6}\cdot 2.3 = 4.2$ nm, from which we estimate an r_{DA} of ∼6 nm (see section 2.4).

Unexpectedly, the relative decrease in fluorescence lifetime, $\langle\tau\rangle_{amp}$ was double that of steady-state fluorescence (25% vs 12%, Figure 2D and Table 2), whereas LY exhibited the opposite tendency, i.e. the steady-state modulation was greater than the relative change in lifetime. The LY observation can be tentatively rationalized by invoking the existence of dark-states.[46,54] In the case of the QD in the oPC state we presume that the complex energy transfer system extends the excited state such that mean acceptor lifetime increases by a factor

Table 2. Properties of LY and QD Emitting Species in Different Preparations[a]

LY	emission wavelength [nm]	QY	quenching [%]	$\langle\tau\rangle_{amp}$ [ns][c]	$\langle\tau\rangle_{amp}$ modulation [%]	cPC/LY in PS state	α_{PS}
psNP	525	0.21	69	1.8 ± 0.3	56	0.67 ± 0.04	0.19
polymersome	529	0.25	20	1.6 ± 0.2	13	0.20 ± 0.02	0.06

QD	emission wavelength [nm]	QY	quenching [%]	$\langle\tau\rangle_{amp}$ [ns][c]	$\langle\tau\rangle_{amp}$ modulation [%]	cPC/QD in PS state	α_{PS}
psNP	640	0.08	12	16.5 ± 0.2	25	35 ± 2	0.19
PMA-QD[b]	640	0.21	–	20.8 ± 0.7	–	–	–

[a]All samples measured in SBB. Excitation for steady-state fluorescence at 420 nm. [b]CdSe/CdS/ZnS 635 nm QDs coated with PMA 75C12 (a polymer which contains only dodecylamine chains). [c]Amplitude-weighed mean fluorescence lifetime. Excitation source, N-460 nanoLED; detection at 525 nm for LY and 635 nm for QD.

dx.doi.org/10.1021/ja3117813 | J. Am. Chem. Soc. 2013, 135, 3208−3217

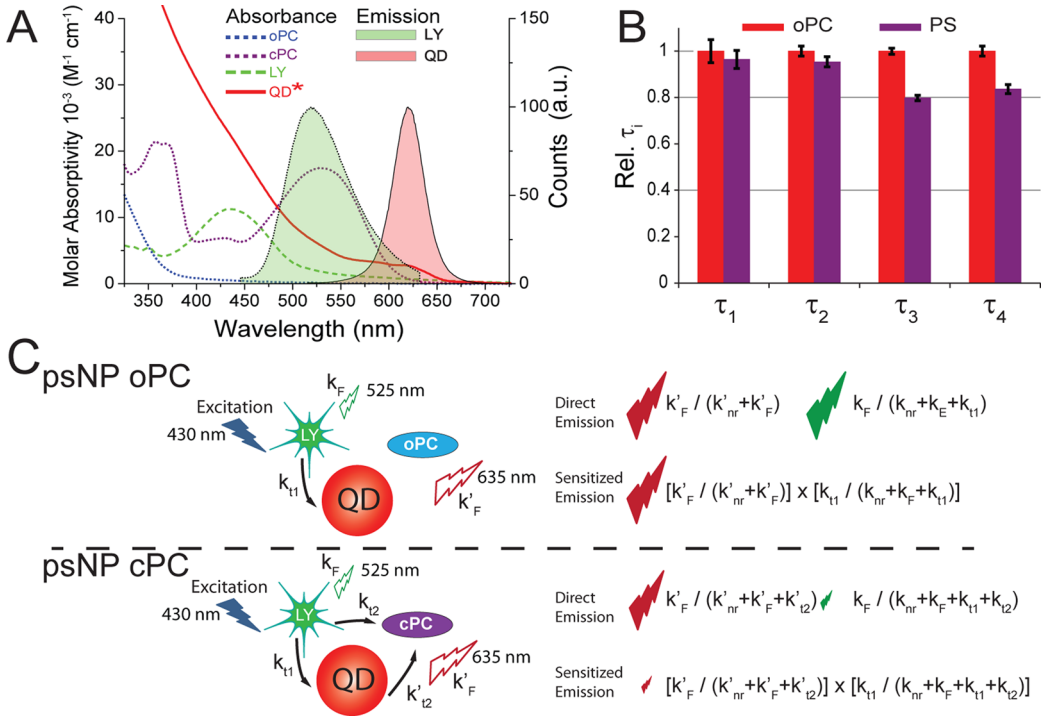

Figure 3. (A) Superposition of absorbance (solid lines) and emission (filled areas) spectra of all the components of the psNP. The emission spectra are normalized by their peak values. *Molar absorptivity of the QD is divided by 100 to fit on the same scale. (B) Individual decay constants of QD emission from psNPs normalized by the values for the oPC state. Absolute decay constants: oPC τ_{1-4}, [0.51; 5.0; 23.5; 55 ns]; PS τ_{1-4}, [0.49; 4.8; 18.8; 46 ns]. (C) Schematic representation of the energy transfer system. LY is denoted as k and QD is denoted as k'. k_F, emission; k_{nr}, nonradiative pathways; k_{t1}, LY to QD energy transfer; k_{t2}, fluorophore to cPC energy transfer. Right side, arrows denoting emission intensities normalized to 100% in the oPC form.

proportional to the transfer efficiency and the donor (LY)/acceptor (QD) ratio. Figure 3 presents a schematic view of the proposed mechanism, the basis of which can be stated as follows. Excitation in the lifetime measurements was at 460 nm, a wavelength at which both fluorophores absorb. LY is capable of acting as a FRET donor to the QD. When the detection is centered at 635 nm, both the direct and sensitized emissions of the QD are registered. However, the lifetime component(s) of the sensitized emission will be longer than those due to direct excitation of the QD.[17,55] When the psNP is at the PS state, the energy transfer from the LY to the QD decreases considerably due to the competing pathway presented by the cPC acceptor (see Figure 3C, specifically k_{t2}). In addition to the decrease in lifetime due to the QD−cPC FRET the QD no longer exhibits the extended lifetime components due to the more prevalent sensitized emission of the oPC state.

Supporting evidence for this hypothesis is observed in the fits to the decay curves of the QD in the psNP. Due to the complex core/shell/shell+polymer shell composition of the psNP, 4 lifetimes (more correctly eigenvalues) were required to accurately fit the data and to determine $\langle\tau\rangle_{amp}$.[35] As is seen in Figure 3B the shorter lifetimes $\tau_{1,2}$ were the same for both states, yet the longer lifetimes $\tau_{3,4}$ decreased by ∼20% in the PS state (exact values are given in the Figure 3 caption). These decay components are the most influenced by sensitized emission pathways. The amplitudes of the individual lifetimes in the two states did not show significant differences.

2.3.3. psNP as Ratiometric Probes. The dual modulations of both fluorophores in psNP do not interfere with its function as a ratiometric imaging particle. Although both emissions decrease in the PS state, the relative changes are quite different. We define an *Emission Ratio* (ER) as the QD emission at 635 nm divided by the LY emission at 525 nm. Upon excitation at 420 nm, there is a >3-fold increase in the ER (4.3 to 13.2, Figure 2B). Figure 4 shows various cycles of psNP through the oPC and PS states generated by alternating UV (lower values) and visible (higher values) irradiation. We observed a slight progressive photobleaching of the LY as the sample was irradiated, reaching 15% after 10 vis−UV cycles. QDs are more photostable than organic dyes and in fact often photobrighten upon cyclical irradiation.[35,56] The LY photobleaching is not a limitation for ratiometric imaging, as can be observed in Figure 4B. The ER change decreased slowly as the psNP was irradiated but the cycle-to-cycle decrease was less than the uncertainty in the measurements.

The mean ER increase was 120 ± 9% with only a 6% decrease due to photobleaching over the course of the 10 cycles.

2.4. Spectral Kinetics and FRET Systems. In addition to the two end states of the psNP, there exists a potentially large number of distinct intermediates differing in cPC content and generated by applying pulses of irradiation. The photoconversion equilibria (α_{PS}) in the 3 systems (polymer in $CHCl_3$, polymersomes, and psNP) were shifted in response to the differences in FRET conditions and degree of intramolecular $\pi-\pi$ interaction (see below), i.e. reflecting the respective donor−acceptor configurations and microenvironments of the PC. The kinetics of photoconversion and quenching were also modified accordingly (Figure 5).

We fit the conversion from oPC to cPC induced by exposure to UV light with an exponential function. The apparent first-order rate constant k'_{oc}[22] was similar for the polymer in $CHCl_3$

dx.doi.org/10.1021/ja3117813 | J. Am. Chem. Soc. 2013, 135, 3208−3217

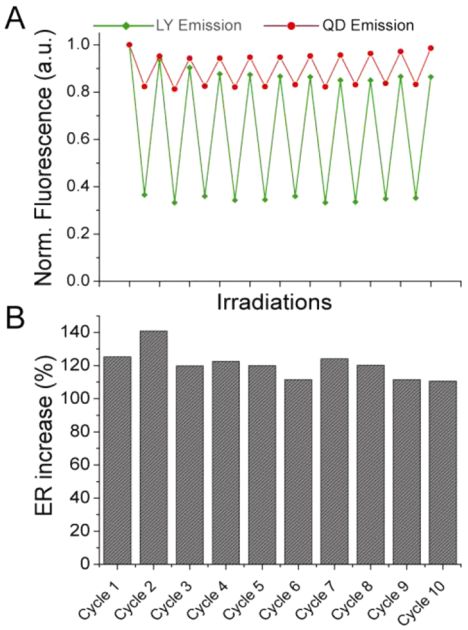

Figure 4. Spectroscopic monitoring of psNP cycled through oPC−PS states. Irradiation was for 150 s; 340 ± 10 nm (1.1 mW cm^{-2}) and 545 ± 10 nm (6.2 mW cm^{-2}). Temperature, 20 °C. (A) Emission of QD (635 nm) and LY (525 nm) after each irradiation, with excitation at 420 nm. (B) Increase in the ER during each cycle upon transition from the oPC to the cPC state.

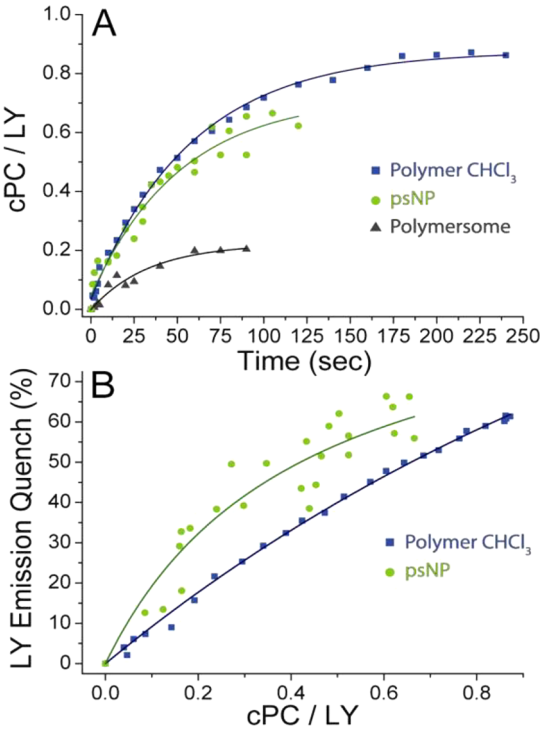

Figure 5. Photoconversion and quenching data (points) and corresponding fits (lines). (A) Graph of the evolution of cPC/LY as a function of UV (1.1 mW cm^{-2}) irradiation time. Fits are monoexponential. (B) Quenching of LY fluorescence as a function of cPC/LY. Fits correspond to eq 1 (polymer) and eq 2 (psNP) from text.

and in the psNP (58 ± 2 and 52 ± 9 s^{-1} respectively), whereas the k'_{oc} for the polymersome was considerably lower (33 ± 9 s^{-1}). We conclude that the local environment created between the QD surface and the polymer cap on a well-formed psNP is similar to that in $CHCl_3$, whereas the polymersomes experience a very different medium. It is important to note that these apparent rate constants also incorporate a contribution representing the cycloreversion of cPC to oPC induced by FRET from either the LY, or the LY and QD in the case of the psNP.[22,25]

The disposition of the LY groups conjugated to PMA in a $CHCl_3$ solution was also examined by time-resolved fluorescent anisotropy. The data were fit[57] to a dual-decay, wobble-in-a-cone model for the dye and a segmental-global rotational depolarization[58] for the polymer, yielding the following parameters: initial anisotropy (r_0), 0.43 ± 0.03; residual anisotropy dye (r_∞), 0.11 ± 0.01; cone half angle (θ), 51 ± 2°; rotational correlation times (ϕ_{dye}, 0.37 ± 0.12 ns; $\phi_{polymer}$, 5.5 ± 0.2 ns). These parameters were invariant during photocycling of PC, the only significant change being a 62% decrease in the amplitude of the longer decay component. The radius of an equivalent sphere of rotation, calculated from the expression $\phi_{rot} = V\eta/kT$ (V, volume; η, solvent viscosity) is 2.1−2.2 nm. For comparison, we estimated the mean-squared radius of gyration of a chainlike polymer, $\langle S_g^2 \rangle = Nl^2\alpha^2/6$, with N, the chain length; l, the monomer lattice length; and α, a factor accounting for excluded volume effects.[59] Chloroform is a good solvent, leading to an expansion of the PMA chain due to favorable polymer−solvent interactions, a phenomenon represented by a value of $\alpha > 1$. The parameters $N = 40$, a corresponding size-dependent $\alpha \approx 1.5$,[59] and $l = 0.52$ nm, lead to an estimate for $\langle S_g^2 \rangle^{1/2}$ of 2.0 nm, in good agreement with the anisotropy data and consistent with PMA existing in $CHCl_3$ as a freely draining dynamic chain with rather mobile pendant LY groups.

The data for the quenching of LY fluorescence as a function of the cPC/LY ratio (Figure 5B) were analyzed with expressions developed for the physical model applicable to each system. In the case of the isolated PMA polymer, the operative FRET equation is given by

$$\text{Quench \%} = 100 \times \left[(1 - e^{-x})\beta x + \sum_{k=1}^{m} \frac{e^{-x}x^k}{k!} \frac{k\gamma}{1 + k\gamma} \right] \quad (1)$$

in which β is a constant and x = cPC/LY; in this particular instance it can also be represented as cPC/polymer. The first term, without which a satisfactory fit was not feasible, accounts for a static quenching of LY by $\pi-\pi$ interactions such as those previously reported for this probe.[54] Stacking would presumably occur preferentially with the cPC form, in view of inherent intramolecular $\pi-\pi$ interaction featured by the parallel configuration of oPC. The second term of eq 1 represents LY-cPC FRET for the population of molecules, assuming a Poisson distribution of the cPC groups. As in the first term of eq 1, quenching occurs only for $k \geq 1$; considering that the values of $x < 1$, $m = 5$ constitutes an adequate upper bound for the distribution. The fit parameters ($\gamma = 15 \pm 7$, $\beta = 0.15 \pm 0.04$) lead to an estimated r_{DA} of 2.6−3.1 nm. As a comparison, we calculated a mean square distance between donor and acceptor units, $\langle r_{DA}^2 \rangle = \langle n \rangle l^2\alpha^2$ with l and α as above, and $\langle n \rangle$ the mean lattice separation of LY donors and cPC acceptors randomly distributed in the PMA;[59] $\langle n \rangle = (N + 1)/3$. The value for r_{DA} calculated in this manner is 2.9 nm, in satisfactory

dx.doi.org/10.1021/ja3117813 | J. Am. Chem. Soc. 2013, 135, 3208−3217

agreement with the fit parameters and also consistent with the flexible chain model.

The corresponding treatment of the psNP quenching by cPC was based on the assumption that the polymers are distributed densely on the surface of the nanoparticle such that intermolecular transfer between LY donors and cPC acceptors conjugated to different polymers can also take place. The psNP configuration is represented as dual concentric shells of acceptor cPC moieties (inner shell, radius r_A) and donor LY (outer shell, radius $r_D = r_A + \Delta r$). Integration of the incremental transfer rate over the entire spherical surface yields the following expression for the FRET efficiency, given as a quenching percentage:

$$\text{Quench } \% = 100 \times \frac{ax}{1 + ax}; \qquad a = p\left(\frac{\delta^2 + 2\delta + 2}{\delta^4(\delta + 2)^4}\right)\mu \tag{2}$$

where $\mu = (R_0/r_A)^6$; $\delta = \Delta r/r_A$; p = LY/psNP = 52 ± 2; and x = cPC/LY. The fit of eq 2 to the psNP data yielded a = 2.44 ± 0.12 and a corresponding set of possible combinations of μ and δ. For R_o = 3.9 nm and r_A = 6.0 nm, δ = 0.58−0.61 from which we calculate an effective outer psNP diameter ($2 \cdot r_D$) of 19.0−19.3 nm. These values are robust, being only 4% lower for an r_A of 5.5 nm, and consistent with the other estimates in this report.

We conclude from the above quantitative considerations that the more facile quenching of psNP at low cPC values, compared to the isolated polymer or polymersomes, is attributable to the increased density and geometric dimensionality of the acceptor population (2D instead of 1D). This circumstance leads to a greater number of potential acceptors per donor and thus the absence of a finite subpopulation devoid of acceptor. In $CHCl_3$ the LY has a higher QY, and the total number of cPC is greater in the PS state, both of which should lead to more efficient energy transfer. However, the parameters of the NP predominate over the polymer such that the observed FRET is higher on the psNPs. In addition, the cPC is sequestered in a different microenvironment of the psNP with little or no possibility for appreciable $\pi-\pi$ static quenching.

3. CONCLUSIONS

We have demonstrated that a nanoparticle template can drastically improve the properties of polymer micelles, creating a new class of psNP that demonstrate many properties of interest as probes in microscopy. The psNP has dual-color emission (525 and 635 nm) with excitation at a single wavelength, small size (~ 20 nm diameter), large modulation of the LY emission both by steady state and time-resolved fluorescence (70% and 55%, respectively), and a mean emission ratio (ER) change of 120%. The carboxyl groups on the surface of the probe potentiate further modifications, for example specific biological targeting of the psNP.[33] The ratiometric modulation should facilitate applications in pulse chase experiments, sensitive lock-in detection strategies,[12,48] and structured illumination schemes such as stochastic optical fluctuation imaging (SOFI).[60,61]

Further improvements can be considered, for example selecting a QD with an emission shifted even further to the red, thus eliminating the overlap of its emission with the PC absorbance. An optimized polymer would have a somewhat higher PC content and a fluorescent probe (FRET donor) with greater photostability and brilliance.

4. EXPERIMENTAL SECTION

4.1. Synthesis of Photochromic Diheteroarylethene. Commercially available Fmoc-L-alanine (64 mg, 205 μmol, Sigma-Aldrich; CAS: 35661-39-3), was added to a flask that had been previously dried and flushed with argon. Thionyl chloride (22 μL, 300 μmol, CAS: 7719-09-7) was added, the flask was flushed with argon, and the reaction was allowed to proceed for 30 min at 50 °C. The flask was dried in a rotovap system to obtain freshly formed (9*H*-fluoren-9-yl)methyl 1-chloro-1-oxopropan-2-ylcarbamate (CAS: 371244-10-9). A solution containing $PCmNH_2$ (50 mg, 100 μmol, [3-(3,3,4,4,5,5-hexafluoro-2-(2-methylbenzo[*b*]thiophen-3-yl)cyclopent-1-enyl)-2-methylbenzo[*b*]thiophen-6-amine]) prepared in the lab[25] was dissolved in dry $CHCl_3$. The solution was added to the dry flask containing the (9*H*-fluoren-9-yl)methyl 1-chloro-1-oxopropan-2-ylcarbamate and allowed to react at 30 °C for 2 h. The reaction was neutralized with NaOH, and the crude product was extracted with CH_2Cl_2; a pink oil was obtained. Purification was performed on a silica gel column with cyclohexane/ethyl acetate (70:30) mobile phase. The intermediate product (9*H*-fluoren-9-yl)methyl 1-(3-(3,3,4,4,5,5-hexafluoro-2-(2-methylbenzo[*b*]thiophen-3-yl)cyclopent-1-enyl)-2-methylbenzo[*b*]thiophen-6-ylamino)-1-oxopropan-2-ylcarbamate was obtained (64 mg, 84 μmol) as a red foam.

The Fmoc protective group was released from the aliphatic amine by addition of excess piperidine (650 μL, 6.5 mmol) in $CHCl_3$ at 50 °C for 20 min. The reaction was quenched with HCl and extracted with CH_2Cl_2. The product was purified by silica gel column, with cyclohexane/THF (30:70) mobile phase. Solvent was evaporated in a rotovap system, and the final product, 2-amino-*N*-(3-(3,3,4,4,5,5-hexafluoro-2-(2-methylbenzo[*b*]thiophen-3-yl)cyclopent-1-enyl)-2-methylbenzo[*b*]thiophen-6-yl)propanamide (29 mg, 52 μmol) was obtained as a yellow/brown oil. ^{1}H NMR (400 MHz, $CDCl_3$, δ) 1.27 (d, 1.05H, CH3 p), 1.29 (s, 1.25H, CH3), 2.17 (*s*, 1.20H, Ar-CH3 ap), 2.20 (s, 1.75H, Ar-CH3 ap), 2.48 (2*s*, 2.40H, Ar-CH3 p), 3.65 (m, 1.07, CH), 6.80−7.70 (m, 6H, ArH), 8.31 (*s*, 0.40H, H-7 ap), 8.35 (*s*, 0.20H, H-7 p), 9.53 (s, 0.30H, Ar-NH-CO), 9.65 (s, 0.51H, Ar-NH-CO). Parallel (p) to antiparallel (ap) conformers 40:60. Exact mass determined by ESI-MS: HRMS (ESI, *m*/*z*): Positive Mode $[M + H]^+$= 555.0982. Calculated mass = 555.0955. HRMS (ESI, *m*/*z*): Negative Mode: $[M]^-$ = 554.0890. Calculated mass = 554.0921.

4.2. Synthesis of Amphiphilic Fluorescent Photomodulatable Polymer. For the polymer synthesis 6 mg (1 μmol polymer, ~40 μmol monomer) of PMA (Sigma-531278, MW ~6,000) was introduced into a dry 10 mL flask. A solution of LYC (Molecular Probes, CAS #149733-79-9, 10 μmol) in DMF (with trace DMSO) was added. The solution was stirred at 60 °C for 90 min and then 9 mg (16 μmol) of PC (see section 4.1) was added in the minimal possible volume of THF. Dodecylamine (2.80 mg, 15 μmol) was added to the flask, and the reaction was left overnight at 60 °C. An additional 2.8 mg (15 μmol) of dodecylamine was added and allowed to react for 6 h. The product was purified and characterized as previously described.[25] The final product is a yellow/orange solid (11 mg).

4.3. psNP Preparation. QD samples (series A CSS 635 nm QDs CdSe/CdS/ZnS core−shell−shell nanoparticles, CAN GmbH, Hamburg) were precipitated from *n*-heptane (solvent supplied by the manufacturer) and resuspended in anhydrous $CHCl_3$. A solution of the photochromic polymer was prepared in anhydrous $CHCl_3$. The solutions were mixed in a glass flask in previously determined optimum proportion (1 mg polymer for 200 pmol of QDs). The reaction was mixed at 65 °C for 2 h. The solvent was evaporated slowly, and once the sample was dry, SBB 50 mM pH 10 was added in excess. The samples were left overnight with mild stirring, and then passed through 0.2 μm inorganic syringe filters. The solution was concentrated to ~1 μM range using Amicon 100 kDa cutoff filters (Millipore) and 50 mM SBB pH 10. Injections of 50 μL were applied to a Superdex 200 analytical column (GE Healthcare Life Science) in an HPLC system. Elution was with 50 mM SBB, pH 9, starting with a flow of 50 μL/min for 3 min and then 20 μL/min. The average run time was 70 min. The psNP peak was collected at 44 min, with empty

dx.doi.org/10.1021/ja3117813 | *J. Am. Chem. Soc.* 2013, 135, 3208−3217

micelles collected at 40 min. In some cases a second chromatographic step was required to obtain optimum purity.

4.4. Sample Irradiation. Samples were irradiated using an Hg arc lamp (SUV-DC, Lumatec, Deisenhofen, Germany) and filters (340 ± 10 nm and 545 ± 10 nm). Samples were placed in Hellma 10 mm × 2 mm or 3 mm × 3 mm microcuvettes, filled such that the entire sample was exposed to light, thereby minimizing inhomogeneities. The samples were kept dilute (<0.1 absorbance at 540 nm for all conversion rates) so as to avoid internal filter effects.

4.5. Measurements. *4.5.1. Absorbance Spectroscopy.* Absorbance spectra (300−800 nm) were acquired on a Cary 100 UV−vis spectrophotometer (Varian) utilizing 100 μL microcuvettes with a 10 mm optical path. A solvent spectrum was utilized as a blank.

4.5.2. Steady-State Fluorescence Spectroscopy. Fluorescence spectra were acquired at 20 °C on a Cary Eclipse fluorescence spectrophotometer (Varian) utilizing Hellma 100 μL microcuvettes. The excitation wavelength was 420 nm when measuring both LY and QD fluorophores and 600 nm for QDs alone. The fluorescence quantum yield (QY) of LY was determined utilizing the known standard Rhodamine 6G in EtOH. For QDs the quantum yield in *n*-heptane was provided by the manufacturer.

4.5.3. Fluorescence Decay and Anisotropy Spectroscopy. Fluorescence lifetime measurements were performed in a Fluoro-Log-TCSPC (Horiba Jobin Yvon). For observing LY, the excitation was carried out with a nanoLED N-460 source (Horiba Scientific) with the emission monochromator set to 525 nm, a time-to-amplitude converter (TAC) range of 50 ns, a pulse repetition frequency of 1 MHz, and a 5,000 counts peak value for automatic timing. For anisotropy measurements polarizers were introduced into the excitation and emission paths. In the case of QD emission, excitation was carried out with a N-460 nanoLED, and the emission monochromator was set to the peak at 635 nm, a TAC range of 500 ns, a pulse repetition frequency of 500 kHz, and 10,000 counts peak value for automatic timing. Data analysis was with laboratory programs implemented with *Mathematica* 8.0 (Wolfram Research).[57]

4.5.4. TEM. Samples of 0.1 μM concentration were prepared in 50 mM SBB buffer, placed on a carbon grid, and imaged with a Philips 120 kV BioTwin microscope equipped with a 1024 × 1024 pixel GATAN CCD camera (Gatan, Inc.); 75−100 particles were measured to calculate diameter statistics.

4.5.5. DLS. Measurements were made with a Nano-ZS Zetasizer nanoseries (Malvern Instruments) and a 90Plus Particle Size Analyzer (Brookhaven Instruments). Solutions were filtered (when appropriate) with 0.2 μm filters and dilutions made with deionized water or buffer solution so as to achieve an optimal concentration. psNP solutions could not be measured in the DLS systems due to the fluorescence of the QD overlapping the laser utilized to detect the sample.

AUTHOR INFORMATION

Corresponding Author

tjovin@gwdg.de

Notes

The authors declare no competing financial interest.

[†]Deceased September 29, 2011.

ACKNOWLEDGMENTS

This article is dedicated to the memory of Elizabeth A. Jares-Erijman. This study was supported by the Max Planck Society (E.J.-E., Partner Group grant; T.M.J and E.J.-E., Toxic Protein Conformation project), Argentine agencies ANpCyT, CONICET, UBA (E.J-E.), and Cluster of Excellence 171 of the DFG Centre for the Molecular Physiology of the Brain (DFG CMPB). S.A.D was supported by the DAAD. We thank D. Arndt-Jovin, V. Shvadchak, D. Yushchenko, and R. Hofele for valuable discussions and suggestions; D. Riedel and G. Heim for the TEM images; Department of Physical Biochemistry, MPIbpc, for the use of the TCSPC fluorimeter; Department of NMR based Structural Biology, MPIbpc for access to NMR spectrometers; Zentrale Analytik, Georg-August-Universität for mass spectrometry.

REFERENCES

(1) Huang, J. G.; Leshuk, T.; Gu, F. X. *Nano Today* **2011**, *6*, 478−492.

(2) Barreto, J. A.; O'Malley, W.; Kubeil, M.; Graham, B.; Stephan, H.; Spiccia, L. *Adv. Mater.* **2011**, *23*, H18−H40.

(3) Mulder, W. J. M.; Strijkers, G. J.; Tilborg, G. A. F. V.; Cormode, D. P.; Fayad, Z. A.; Nicolay, K. *Acc. Chem. Res.* **2009**, *42*, 904−914.

(4) Hahn, M. A.; Singh, A. K.; Sharma, P.; Brown, S. C.; Moudgil, B. M. *Anal. Bioanal. Chem.* **2010**, *399*, 3−27.

(5) Byers, R. J.; Hitchman, E. R. *Prog. Histochem. Cytochem.* **2011**, *45*, 201−237.

(6) Chan, Y.-H.; Ye, F.; Gallina, M. E.; Zhang, X.; Jin, Y.; Wu, I. C.; Chiu, D. T. *J. Am. Chem. Soc.* **2012**, *134*, 7309−7312.

(7) Bigall, N. C.; Parak, W. J.; Dorfs, D. *Nano Today* **2012**, *7*, 282−296.

(8) Cheon, J.; Lee, J.-H. *Acc. Chem. Res.* **2008**, *41*, 1630−1640.

(9) Barroso, M. M. *J. Histochem. Cytochem.* **2011**, *59*, 237−251.

(10) Credi, A. *New J. Chem.* **2012**, *36*, 1925−1930.

(11) Agasti, S. S.; Kohler, R. H.; Liong, M.; Peterson, V. M.; Lee, H.; Weissleder, R. *Small* **2013**, *9*, 222−227.

(12) Marriott, G.; Mao, S.; Sakata, T.; Ran, J.; Jackson, D. K.; Petchprayoon, C.; Gomez, T. J.; Warp, E.; Tulyathan, O.; Aaron, H. L.; Isacoff, E. Y.; Yan, Y. *Proc. Natl. Acad. Sci. U.S.A.* **2008**, *105*, 17789−17794.

(13) Tian, Z.; Wu, W.; Wan, W.; Li, A. D. Q. *J. Am. Chem. Soc.* **2009**, *131*, 4245−4252.

(14) Willig, K. I.; Stiel, A. C.; Brakemann, T.; Jakobs, S.; Hell, S. W. *Nano Lett.* **2011**, *11*, 3970−3973.

(15) Li, A. D. Q.; Zhan, C. L.; Hu, D. H.; Wan, W.; Yao, J. N. *J. Am. Chem. Soc.* **2011**, *133*, 7628−7631.

(16) Jares-Erijman, E. A.; Jovin, T. M. *Nat. Biotechnol.* **2003**, *21*, 1387−1395.

(17) Algar, W. R.; Wegner, D.; Huston, A. L.; Blanco-Canosa, J. B.; Stewart, M. H.; Armstrong, A.; Dawson, P. E.; Hildebrandt, N.; Medintz, I. L. *J. Am. Chem. Soc.* **2012**, *134*, 1876−1891.

(18) Menendez, G. O.; Pichel, M. E.; Spagnuolo, C. C.; Jares-Erijman, E. A. *Photochem. Photobiol. Sci.* **2013**, *12*, 236−240.

(19) Hofmann, M.; Eggeling, C.; Jakobs, S.; Hell, S. W. *Proc. Natl. Acad. Sci. U.S.A.* **2005**, *102*, 17565−17569.

(20) Davis, C. M.; Childress, E. S.; Harbron, E. J. *J. Phys. Chem. C* **2011**, *115*, 19065−19073.

(21) Yildiz, I.; Deniz, E.; Raymo, F. M. *Chem. Soc. Rev.* **2009**, *38*, 1859−1867.

(22) Giordano, L.; Jovin, T. M.; Irie, M.; Jares-Erijman, E. A. *J. Am. Chem. Soc.* **2002**, *124*, 7481−89.

(23) Zhang, J.; Zou, Q.; Tian, H. *Adv. Mater.* **2013**, *25*, 378−399.

(24) Jares-Erijman, E.; Giordano, L.; Spagnuolo, C.; Lidke, K.; Jovin, T. *Mol. Cryst. Liq. Cryst.* **2005**, *430*, 257−265.

(25) Díaz, S. A.; Menendez, G. O.; Etchehon, M. H.; Giordano, L.; Jovin, T. M.; Jares-Erijman, E. A. *ACS Nano* **2011**, *5*, 2795−2805.

(26) Irie, M. *Photochem. Photobiol. Sci.* **2010**, *9*, 1535−1542.

(27) Saitoh, M.; Fukaminato, T.; Irie, M. *J. Photochem. Photobiol., A* **2009**, *207*, 28−31.

(28) Genovese, D.; Montalti, M.; Prodi, L.; Rampazzo, E.; Zaccheroni, N.; Tosic, O.; Altenhöner, K.; May, F.; Mattay, J. *Chem. Commun.* **2011**, *47*, 10975−10977.

(29) Osakada, Y.; Hanson, L.; Cui, B. *Chem. Commun.* **2012**, *48*, 3285−3287.

(30) Chen, J. A.; Zhang, P. S.; Yu, X. Y.; Li, X. F.; Tao, H. W.; Yi, P. G. *J. Macromol. Sci., Pure Appl. Chem.* **2011**, *48*, 219−226.

(31) Cusido, J.; Battal, M.; Deniz, E.; Yildiz, I.; Sortino, S.; Raymo, F. M. *Chem.—Eur. J.* **2012**, *18*, 10399−10407.

(32) Edelsztein, V. C.; Jares-Erijman, E. A.; Mullen, K.; Di Chenna, P. H.; Spagnuolo, C. C. *J. Mater. Chem.* **2012**, *22*, 21857−21861.

(33) Sperling, R. A.; Parak, W. J. *Philos. Trans. R. Soc., A* **2010**, *368*, 1333−1383.
(34) Pellegrino, T.; Manna, L.; Kudera, S.; Liedl, T.; Koktysh, D.; Rogach, A. L.; Keller, S.; Rädler, J.; Natile, G.; Parak, W. J. *Nano Lett.* **2004**, *4*, 703−707.
(35) Díaz, S. A.; Giordano, L.; Jovin, T. M.; Jares-Erijman, E. A. *Nano Lett.* **2012**, *12*, 3537−44.
(36) Discher, D. E.; Eisenberg, A. *Science* **2002**, *297*, 967−973.
(37) Zhou, K.; Liu, H.; Zhang, S.; Huang, X.; Wang, Y.; Huang, G.; Sumer, B. D.; Gao, J. *J. Am. Chem. Soc.* **2012**, *134*, 7803−7811.
(38) Tong, R.; Hemmati, H. D.; Langer, R.; Kohane, D. S. *J. Am. Chem. Soc.* **2012**, *134*, 8848−8855.
(39) Zhu, M. Q.; Zhu, L.; Han, J. J.; Wu, W.; Hurst, J. K.; Li, A. D. Q. *J. Am. Chem. Soc.* **2006**, *128*, 4303−4309.
(40) Zhu, L.; Wu, W.; Zhu, M.-Q.; Han, J. J.; Hurst, J. K.; Li, A. D. Q. *J. Am. Chem. Soc.* **2007**, *129*, 3524−3526.
(41) Janczewski, D.; Tomczak, N.; Han, M.-Y.; Vancso, G. J. *Nat. Protoc.* **2011**, *6*, 1546−53.
(42) Hu, G. H.; Lindt, J. T. *Polym. Bull.* **1992**, *29*, 357−363.
(43) Sperling, R. A.; Pellegrino, T.; Li, J. K.; Chang, W. H.; Parak, W. J. *Adv. Funct. Mater.* **2006**, *16*, 943−948.
(44) Murakami, M.; Miyasaka, H.; Okada, T.; Kobatake, S.; Irie, M. *J. Am. Chem. Soc.* **2004**, *126*, 14764−14772.
(45) Kwon, D.-H.; Shin, H.-W.; Kim, E.; Boo, D. W.; Kim, Y.-R. *Chem. Phys. Lett.* **2000**, *328*, 234−243.
(46) Sillen, A.; Engelborghs, Y. *Photochem. Photobiol.* **1998**, *67*, 475−486.
(47) Mishra, P. P.; Koner, A. L.; Datta, A. *Chem. Phys. Lett.* **2004**, *400*, 128−132.
(48) Petchprayoon, C.; Yan, Y. L.; Mao, S.; Marriott, G. *Bioorg. Med. Chem.* **2011**, *19*, 1030−1040.
(49) Borst, J. W.; Visser, A. *Meas. Sci. Technol.* **2010**, *21*, 102002.
(50) Evans, C. M.; Love, A. M.; Weiss, E. A. *J. Am. Chem. Soc.* **2012**, *134*, 17298−17305.
(51) Talapin, D. V.; Mekis, I.; Götzinger, S.; Kornowski, A.; Benson, O.; Weller, H. *J. Phys. Chem. B* **2004**, *108*, 18826−18831.
(52) Sperling, R. A.; Liedl, T.; Duhr, S.; Kudera, S.; Zanella, M.; Lin, C. A. J.; Chang, W. H.; Braun, D.; Parak, W. J. *J. Phys. Chem. C* **2007**, *111*, 11552−11559.
(53) Métivier, R.; Badré, S.; Méallet-Renault, R.; Yu, P.; Pansu, R. B.; Nakatani, K. *J. Phys. Chem. C* **2009**, *113*, 11916−11926.
(54) Fürstenberg, A.; Vauthey, E. *Photochem. Photobiol. Sci.* **2005**, *4*, 260−267.
(55) Xu, H.; Huang, X.; Zhang, W.; Chen, G.; Zhu, W.; Zhong, X. *ChemPhysChem* **2010**, *11*, 3167−3171.
(56) Carrillo-Carrion, C.; Cardenas, S.; Simonet, B. M.; Valcarcel, M. *Chem. Commun.* **2009**, 5214−5226.
(57) Celej, M. S.; Jares-Erijman, E. A.; Jovin, T. M. *Biophys. J.* **2008**, *94*, 4867−4879.
(58) Gradinaru, C. C.; Marushchak, D. O.; Samim, M.; Krull, U. J. *Analyst* **2010**, *135*, 452−459.
(59) Belfiore, L. A. In *Physical Properties of Macromolecules*; John Wiley & Sons, Inc.: New York, 2010; pp 547−607.
(60) Dertinger, T.; Colyer, R.; Iyer, G.; Weiss, S.; Enderlein, J. *Proc. Natl. Acad. Sci. U.S.A.* **2009**, *106*, 22287−22292.
(61) Dedecker, P.; Mo, G. C.; Dertinger, T.; Zhang, J. *Proc. Natl. Acad. Sci. U.S.A.* **2012**, *109*, 10909−10914.